A computational study on the electrified Pt(111) surface by the cluster model

Jian Yang

Science Institute, University of Iceland, Dunhagi 3, 107 Reykjavík, Iceland

E-mail: jianyang@hi.is

Supplementary information

For the Pt_{37} cluster system, the conceptions of the constant potential method has been introduced and discussed by Auer et al. in comparisons with the neutral charge method, and the relevant formulas to calculate the adsorption energy and reaction enthalpy in those methods have been elucidated with details.[1] The relevant expressions for NO adsorption and reduction on Pt_{37} cluster are described in the following equations, where the Pt(111) surface of the Pt_{37} cluster and the hydrogenated intermediate are denoted as * and P. As the conventional approach in thermochemistry computation, the neutral (constant) charge method for NO adsorption and reduction can be described in eqn (SI-1) and (SI-3), respectively. The proton and electron couple can be simulated by the computational hydrogen electrode. In the constant potential method, the total charges of the initial and the final states of the cluster system have to be considered during the surface process, i.e. NO adsorption (eqn (SI-2)) and reduction (eqn (SI-4)), during which the initial and the final charge states are denoted by superscript t and m, respectively. Therefore, the overall flux of the partial charge $(m-t)e^-$ is required to fix the potential.

$$NO + * \rightarrow *NO \quad \text{(SI-1)}$$

$$NO + *^t \rightarrow (*NO)^m + (m-t)e^- \quad \text{(SI-2)}$$

$$NO + * + n(H^+ + e^-) \rightarrow *P \quad \text{(SI-3)}$$

$$NO + *^t + n(H^+ + e^-) \rightarrow (*P)^m + (m-t)e^- \quad \text{(SI-4)}$$

The free energy of the reaction species on the Pt_{37} cluster has been calculated with the energy corrections according to eqn (SI-5). The electronic energy E_{el} includes the dispersion and the dipole corrections. E_{ZPE}, E_{vib}, E_{rot} and E_{trans} are the zero-temperature vibrational energy, the vibrational energy correction at room temperature, the rotational thermal energy and the translational thermal energy respectively, and k_B is the Boltzmann's constant. The total entropy S_{tot} summarizes the electronic entropy, vibrational entropy, rotational entropy and translational entropy, respectively. Those energy corrections can be obtained directly by the numerical frequency computation in the ORCA program. For all computations of the Pt_{37} cluster system performed with ORCA program, the convergence criteria are 1.0e-8 E_h and 1.0e-5 E_h for the energy change and the orbital gradient, respectively.

$$G = E_{el} + E_{ZPE} + E_{vib} + E_{rot} + E_{trans} + k_BT - TS_{tot} \quad \text{(SI-5)}$$

In the constant potential method, the Pt_{37} cluster system has been calculated in different charge states from -2 to 2, and the relevant Fermi level of the cluster system can be applied to find out the corresponding potential. Consequently, the grand canonical energy of the Pt_{37} cluster system can be obtained as a function of the potential as discussed by Auer and co-workers.[1] Each surface intermediate during NO

reduction on the Pt_{37} cluster has been calculated in the same functional and basis set, so that the reaction energies can be calculated in the same potential for the surface intermediates. This strategy is also applied in the computations of the potential-dependent activation energy.

In Fig. S1, there are different trends about adsorption energy varying along the total charge between the top and the threefold-hollow sites. When the CPCM model is applied, adsorption energy slightly decreases in the whole range of total charge, and gradually shifts negatively as the total charge becomes positively.

The potential dependence of H, OH and O adsorption on the Pt(111) surface of the Pt_{37} cluster are briefly studied with adsorbate covered surfaces at the PBE+D3 level of theory. The potential for the relevant reaction is calculated conceptually according to the standard state of 1M Pt_{37} nanoparticle with adsorbate and 1M bare Pt_{37} nanoparticle. The most stable states of those species on the Pt(111) surface have been plotted in the free energy profiles as a function of the potential variation. Therefore, the potential-dependent free energy profile reflects the thermochemistry of the surface reaction. For H adsorption, the top site is more favorable than other sites on the Pt(111) surface of the Pt_{37} cluster by the two methods. Those obtained in the constant potential method are shown in Fig. S2. Without the implicit solvation model, the onset potential of H adsorption is predicted as positive as ca. 0.63 V, and those of OH and O adsorptions on the Pt(111) surface are ca. 0.45 V and 0.62 V, respectively. When the CPCM model is applied, the onset potential of H adsorption shifts down to ca. 0 V, and those of OH and O adsorptions shift positively to ca. 0.58 V and 0.70 V, respectively. Therefore, the double-layer range can be assigned between the onset potentials of H and OH adsorption.

The relevant free energy profiles obtained in the neutral charge method are shown in Fig. S3. The CPCM model only shows a limited influence on the onset potential of H adsorption, and double-layer range is still overwhelmed by H and OH adsorptions. Although H underpotential adsorption on Pt(111) surface in experiments cannot be included in those simulations, the onset potential of H adsorption is positively overestimated in Fig. S2(a) and Fig. S3. Moreover, the onset potentials predicted from the constant potential method with the CPCM model are comparable to those obtained in the infinite system using the explicit solvation model.[2] Since the local solvation details on surface adsorbates are completely omitted, it is not possible to reproduce the corresponding voltammogram features in experiments, for instance those in perchloric acid. However, the qualitative features of the predicted onset potentials can be comparable to those in experiments. Therefore, the constant potential method combined with the CPCM model can provide more proper prediction of onset potential rather than the other methods. This combination has been applied to investigate the onset potential of H adsorption on the CN and the NO pre-adsorbed Pt(111) surface, respectively, as shown in Fig. S4.

For NO reduction on the Pt(111) surface of the Pt_{37} cluster, the Pt_{37} cluster system is large enough to render the qualitative trends of the free energy profiles that are comparable to the relevant results obtained in the infinite model using the neutral charge method. The relevant free energy profiles in the constant charge method are analogous to those in the neutral charge method (Fig. S6). In general, the free energy

for each surface intermediate changes to a limited extent as the total charge of the cluster varies; NOH on Pt(111) surface is ca. 1.38 kcal mol^{-1} and 1.16 kcal mol^{-1} more stable than HNO when the total charge of the cluster is -2 and 2, respectively. The total charge of the cluster system is kept constant along the reaction coordinate in those two methods, and the potential differences between the surface intermediates during the surface reactions cannot be considered in those computations. Therefore, the change in the free energy for each surface intermediate is trivial between different charge states of the cluster system in this study. In the constant potential method, the thermochemical stability of the key intermediate on the Pt(111) surface changes significantly along the potential variation in Fig. 7. In lower potential range, NOH on the Pt(111) surface is found out to be more stable than HNO, which is consistent with the qualitative trend in the neutral charge method (Fig. 5). However, in the constant potential method, HNOH on the Pt(111) surface becomes more stable than H_2NO in a wide potential range. This is contrary to the thermochemical stability in the neutral charge method for the second elementary step reaction. For the third elementary step, NH radical on the Pt(111) surface is more stable than NH_2OH in the neutral charge and the constant potential methods. The reaction from the N atom to NH radical on the Pt(111) surface is endergonic in the constant potential method between 0 V and 0.84 V. This reaction in the neutral charge method is exergonic at 0 V and 0.32 V (Fig. 5 (b) and Fig. S5 (c)), whereas it becomes endergonic at 0.84 V (Fig. S5 (d)). In the neutral charge and the constant potential methods, the thermochemistry on the elementary steps of NH radical reduction to NH_3 on the Pt(111) surface depends on the potential, and the free energies of those reactions change in different trends along the potential variation in the range. In Fig. S7, S8, S9, S10, Table 6 and 7, the subscripts t, f, h and b, respectively, stand for the top, the fcc, the hcp and the bridge sites of the Pt(111) surface on the Pt_{37} cluster; for the same kind of adsorption site, the number indicates a different part of the Pt(111) surface or different orientation on the surface. In Fig. S8, the slope of free energy varying along the potential can be treated in a linear fitting. They are 0.994 e (± 5.46e-5, Adj. R^2=1) and 0.989 e (± 9.80e-5, Adj. R^2=1), respectively, for NOH and HNO at the most stable sites. Those are ascribed to a lower charge capacity in the potential scaling without the CPCM model. Consequently, the free energy difference between NOH and HNO at the most stable sites scarcely changes along the potential; it is ca. 1.90 kcal mol^{-1} steadily in the whole potential range.

The CPCM model does not influence the activation energy related to the LH mechanism in the neutral charge method as shown in Fig. S11. When ZPE energy correction in the gas phase is included, the activation energies of HNO at the top site are ca. 15.58 kcal mol^{-1} and 15.21 kcal mol^{-1} without and with the CPCM model, respectively; whereas those of NOH at the fcc site are ca. 30.23 kcal mol^{-1} and 31.19 kcal mol^{-1} in the corresponding conditions. The surface reactions via the ER mechanism are studied with the CPCM model. The relevant images about NOH and HNO formation are shown in Fig. S13. The first transition states are related to the O-H and N-H bond formations in the corresponding reaction paths. This step regenerates the water molecule that maintains a hydrogen bond above the Pt(111) surface. The second ones correspond to the diffusion of the water molecule before its final adsorption on the Pt(111) surface.

The localized MOs in the Pipek-Mezey method for isomeric intermediates in the gas phase are shown in Fig. 11. For triplet NOH, there are three strongly localized alpha SOMOs of the O and the N sites and a π bond-like localized beta SOMO polarizing mainly to the side of O site (O: 0.812 and N: 0.182). For triplet NO^-, there are strongly localized alpha SOMOs of the O and the N site and π bond-like localized beta SOMOs between the N and the O sites with polarization to the N site (O: 0.693 and N: 0.307). The localized SOMOs of ground-state isomeric intermediates on the Pt(111) surface are shown in Fig. 12. For NOH at the top site, there is a pair of σ bond-like localized SOMOs related to the N-Pt bond, which are alpha (N: 0.427 and Pt: 0.588) and beta (N: 0.558 and Pt: 0.466) orbitals; moreover, there are a bond-like localized beta SOMO between the N and the Pt sites with negligible polarization to the Pt site (N: 0.862 and Pt: 0.091), a strongly localized SOMO of the O site and a π bond-like localized alpha SOMO between the N and the O sites (O: 0.803 and N: 0.170). For NOH at the fcc site, there is a pair of σ bond-like localized SOMOs related to one N-Pt bond, which are alpha (N: 0.472 and Pt: 0.487) and beta (N: 0.298 and Pt: 0.636) orbitals; there is a pair of more delocalized orbitals associated with two N-Pt bonds, which are alpha (Pt: 0.170, Pt: 0.081 and N: 0.665) and beta (Pt: 0.082, Pt: 0.082 and N: 0.655) orbitals; there is more delocalized beta SOMO associated with one N-Pt bond (Pt: 0.757 and N: 0.075). For HNO at the top site, the pair of σ bond-like localized SOMOs associated with N-Pt bond are alpha (N: 0.691 and Pt: 0.417) and beta (N: 0.724 and Pt: 0.363) orbitals.

The adsorption energy in the thermochemical cycle to calculate the surface pK_{a*} is defined for the acid and the conjugated base in the following equations:

$$\Delta G^\circ_{ads,\,A^-} = G^\circ_{sol,\,*A^-} - G^\circ_{sol,\,*} - G^\circ_{sol,\,A^-} \quad \text{(SI-6)}$$

$$\Delta G^\circ_{ads,\,HA} = G^\circ_{sol,\,*AH} - G^\circ_{sol,\,*} - G^\circ_{sol,\,HA} \quad \text{(SI-7)}$$

In Table S5, the indirect approach is to apply the thermochemical cycle in the same strategy to the surface pK_a* computation, and the adsorption energy of NO^- on the Pt(111) surface is taken as that of NOH. The direct approach is based on the free energy difference between NO_{ads} and the surface intermediates in the constant potential method combined with the CPCM model.

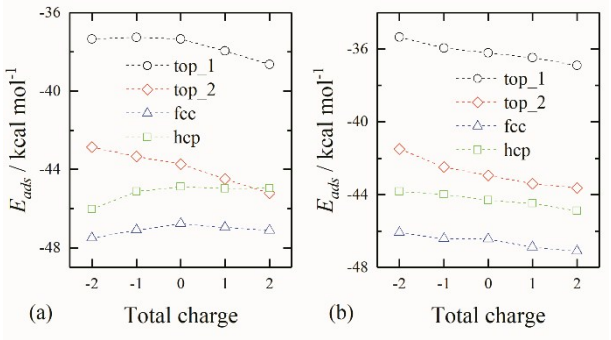

Fig.S1 NO adsorption energy on the Pt(111) surface of the Pt_{37} cluster at different total charge (a) without and (b) with the CPCM model.

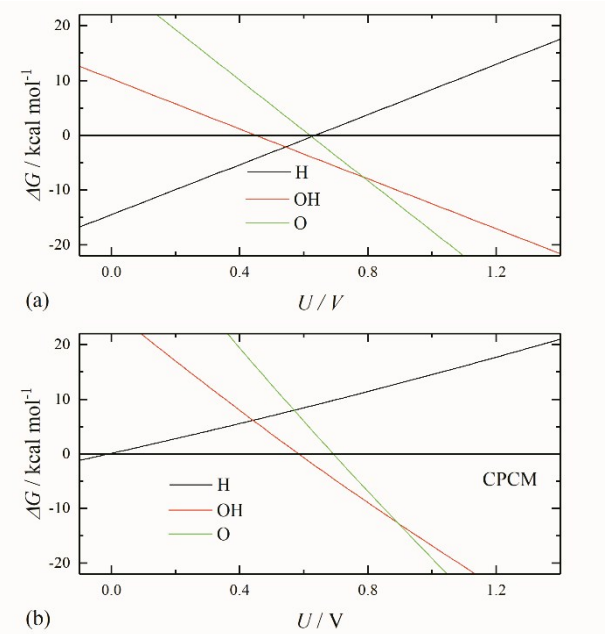

Fig. S2 Free energy profiles of H, OH and O adsorptions on the Pt(111) surface of the Pt_{37} cluster as a function of the potential in the constant potential method (a) without and (b) with the CPCM model.

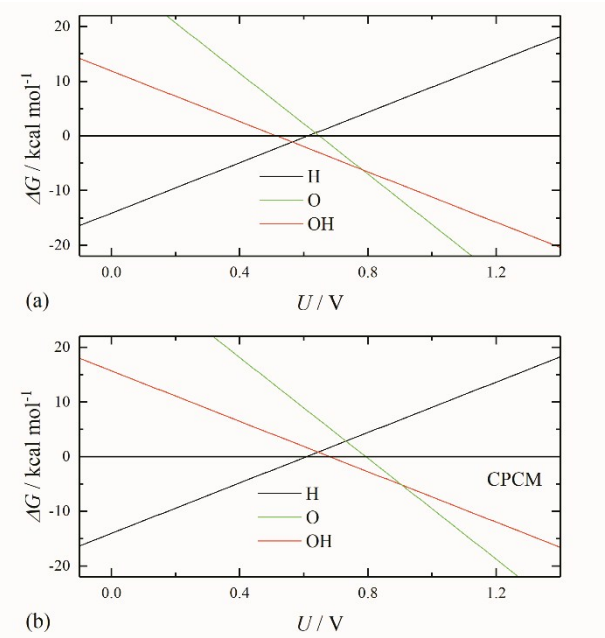

Fig. S3 Free energy profiles of H, OH and O adsorptions on the Pt(111) surface of the Pt_{37} cluster as a function of the potential in the neutral charge method (a) without and (b) with the CPCM model.

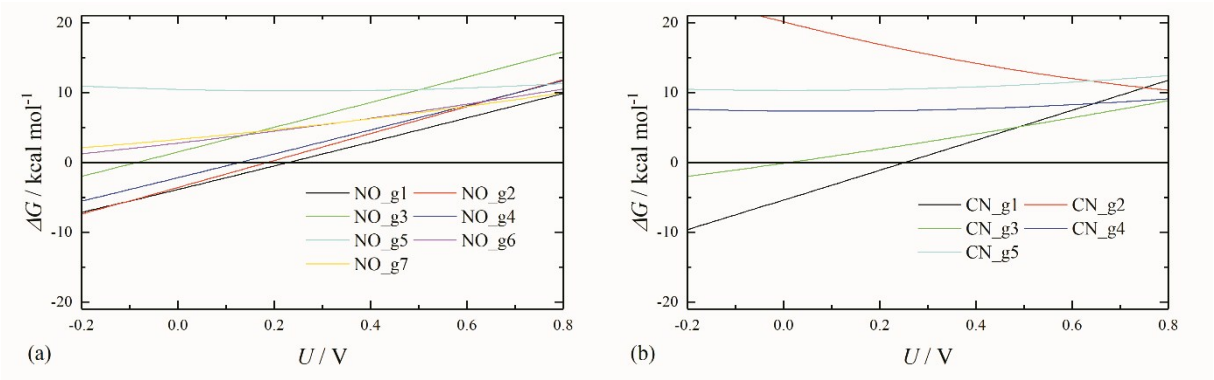
20
10
0
-10
-20
-0.2
0.0
0.2
0.4
0.6
0.8
ΔG / kcal mol-1
U / V
(a)
NO_g1
NO_g2
NO_g3
NO_g4
NO_g5
NO_g6
NO_g7
(b)
CN_g1
CN_g2
CN_g3
CN_g4
CN_g5

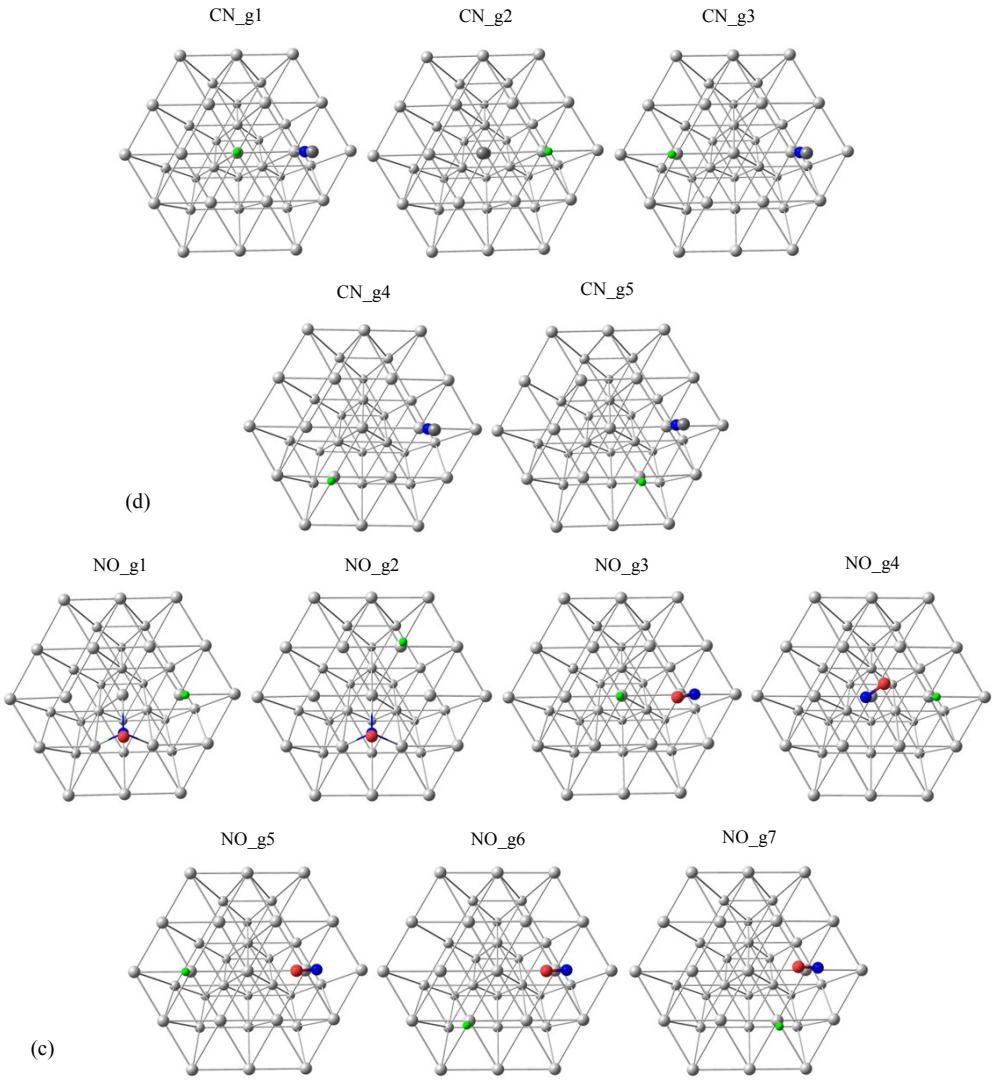

Fig. S4 Free energy profiles of H adsorption as a function of the potential in the constant potential method combined with the CPCM model when (a) NO and (b) CN are spectators on the Pt(111) surface of the Pt_{37} cluster, respectively. Top views of the geometries of H+NO and H+CN on the Pt(111) surface are listed in (c) and (d), respectively, and the color of H atom is emphasized in green.

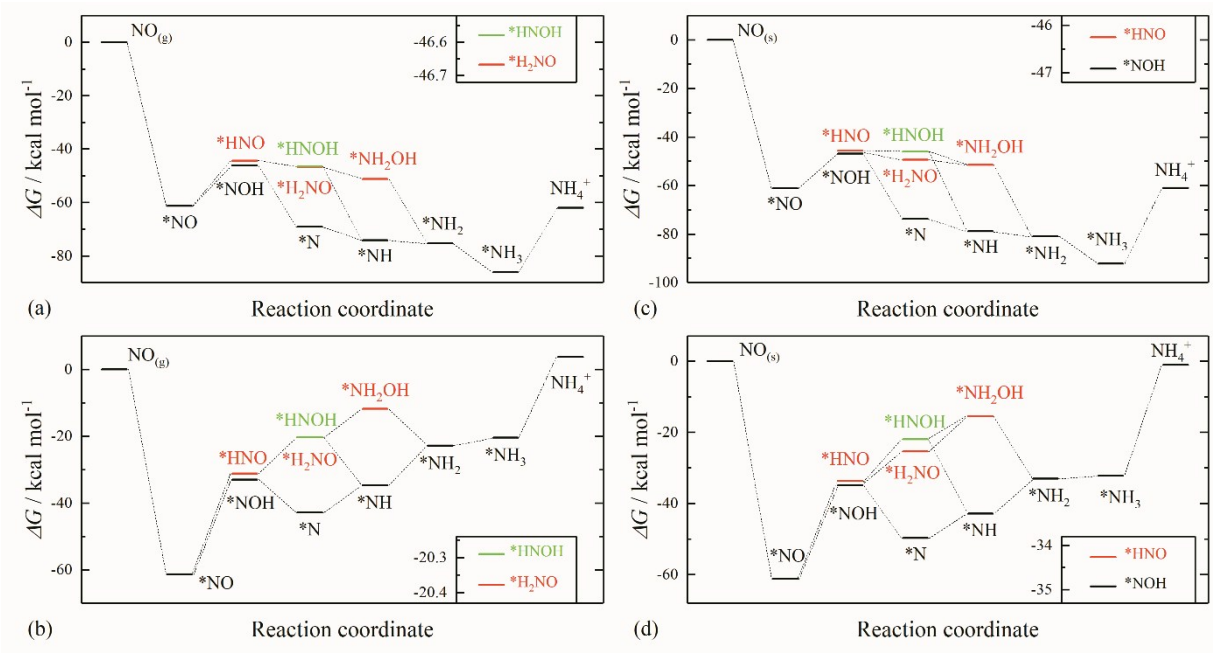

Fig. S5 Free energy profiles for NO reaction to NH_4^+ on the Pt(111) surface of the Pt_{37} cluster in the neutral charge method without the CPCM model at (a) 270 mV and (b) 840 mV, and combined with the CPCM model at (c) 320 mV and (d) 840 mV.

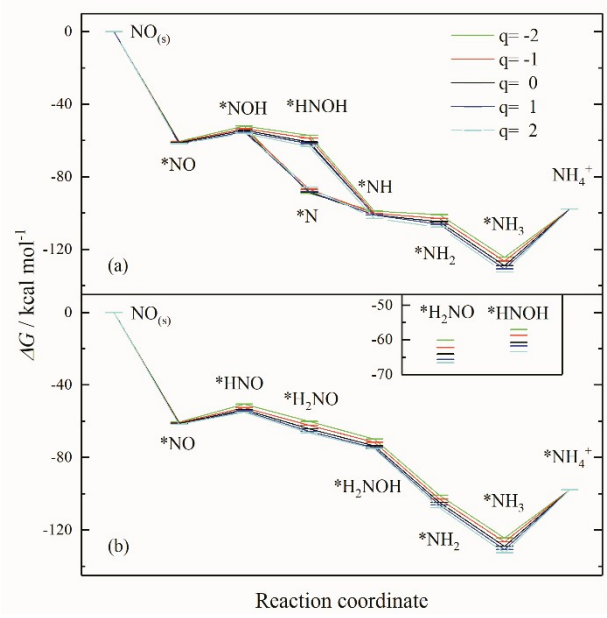

Fig. S6 Free energy profiles of NO reduction to NH_4^+ on the Pt(111) surface of the Pt_{37} cluster in the constant charge method combined with the CPCM model at 0 V. The total charges (q) are indicated by different colours. The reaction pathways via NOH and HNO are shown in (a) and (b), respectively. Since the energies for the surface intermediates HNOH and H_2NO are too close, they are compared in a separate inset within (b).

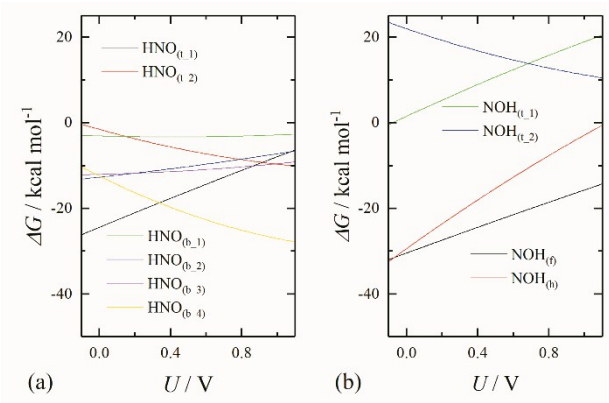

Fig. S7 Potential dependence of free energy profiles in the constant potential method with the CPCM model for (a) HNO and (b) NOH at the different sites of the Pt(111) surface.

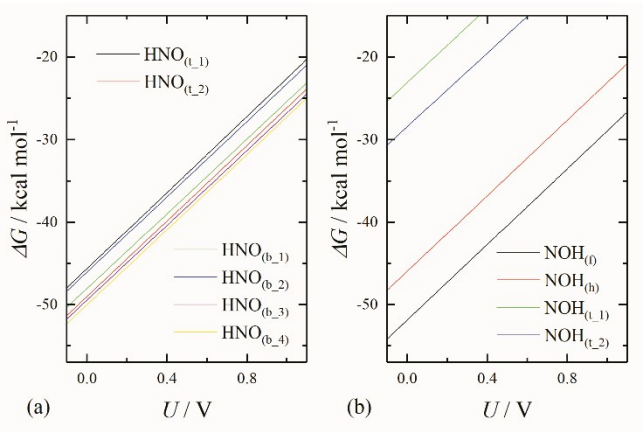

Fig. S8 Potential dependence of free energy profiles in the constant potential method without the CPCM

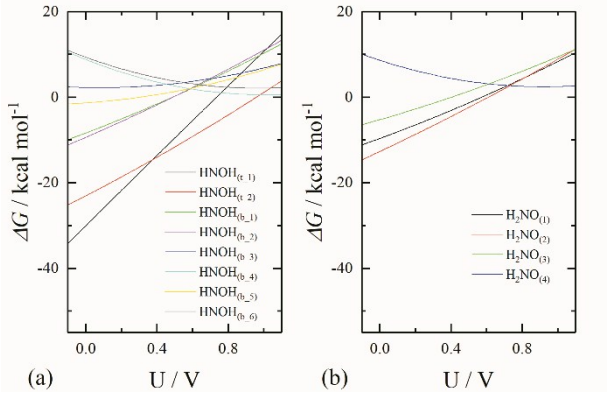

model for (a) HNO and (b) NOH at the different sites of the Pt(111) surface.

Fig. S9 Potential dependence of free energy profiles in the constant potential method with the CPCM model for (a) HNOH and (b) H_2NO at the different sites of the Pt(111) surface.

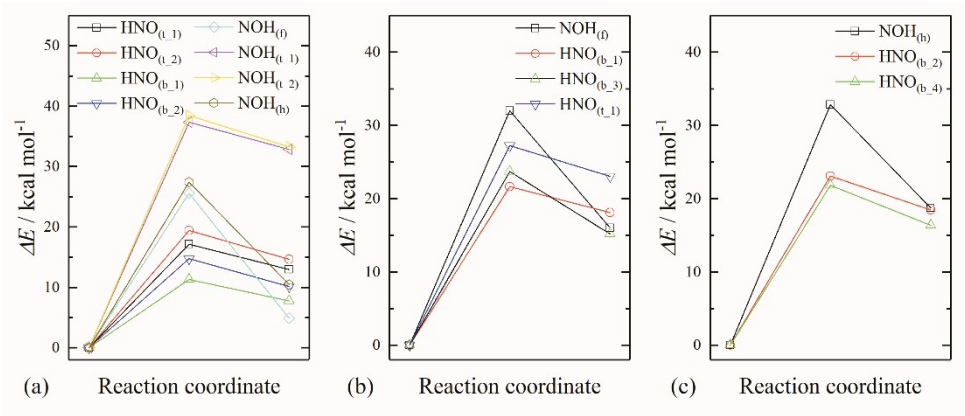

Fig. S10 Energy variation along the reaction coordinate via the LH mechanism between H_{ads} and NO_{ads} at (a) the top, (b) the fcc and (c) the hcp sites on the Pt(111) surface of the Pt_{37} cluster in the neutral charge method without the CPCM model. The energies of reactants are taken as 0, and the middle of reaction coordinate is related to the transition state.

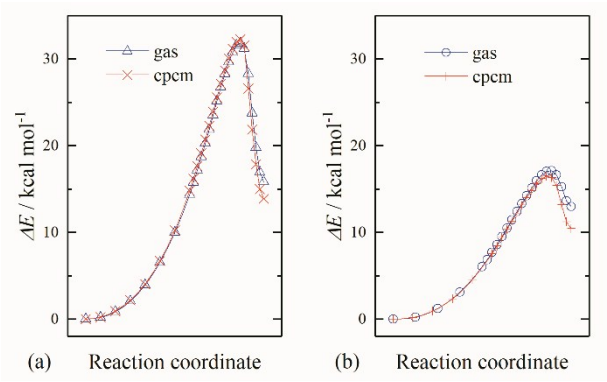

Fig. S11 Energy variation along the reaction coordinate via the LH mechanism without (gas) and with the CPCM model in the neutral charge method: (a) NOH formation at the same fcc site, and (b) HNO formation at the same top site on the Pt(111) surface of the Pt_{37} cluster.

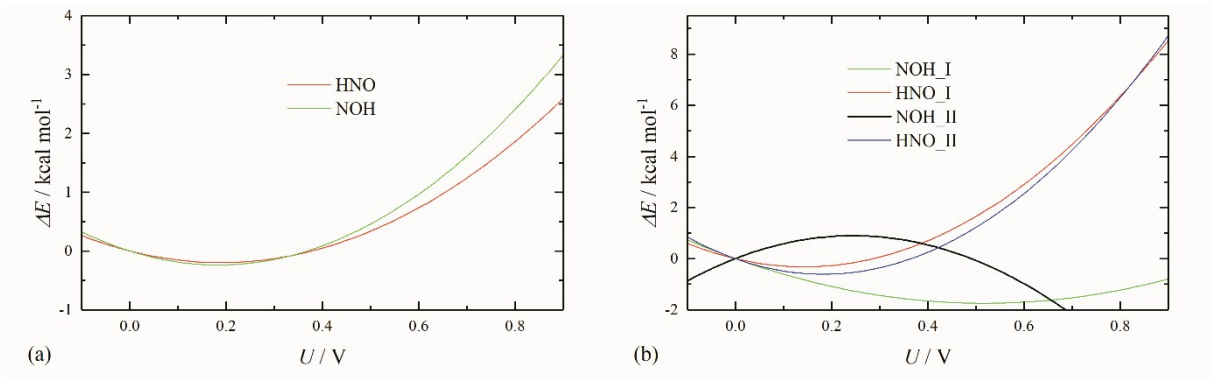

Fig. S12 Activation energies contributed from the flux of the partial charge in the constant potential method for NOH and HNO formations via (a) the LH and (b) the ER mechanisms.

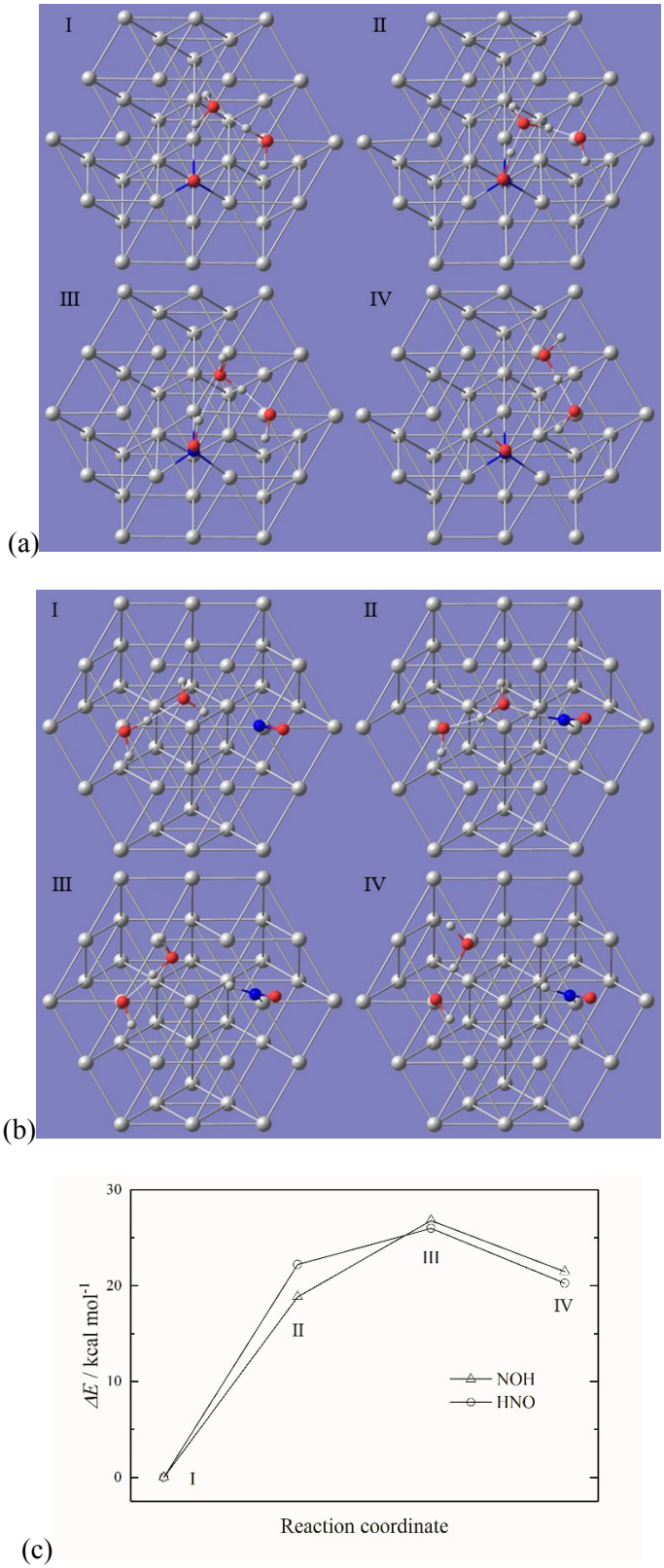

Fig. S13 Images of the initial (I), transition (II and III) and final states (IV) for NO_{ads} reduction to (a) NOH at the same fcc site and (b) HNO at the same top site via the ER mechanism, and (c) the energy variation against the initial state along the reaction coordinate when the total charge of the cluster system is -1.

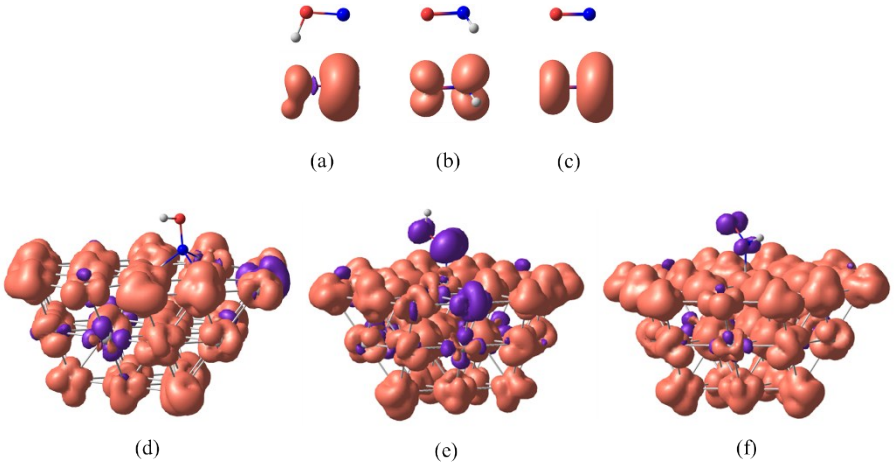

Fig. S14 Spin densities of isomeric intermediates in the gas phase and on the Pt_{37} cluster: (a) triplet NOH, (b) doublet HNO^- and (c) triplet NO^- anion, (d) ground-state NOH at the fcc site, (e) ground-state NOH at the top site, and (f) ground-state HNO at the top site of the Pt(111) surface. Isosurfaces have been obtained at the B3LYP/def2-TZVP level of theory with the corresponding diffuse basis set for anion species. The contour is 0.005.

Table S1 Data about the free energy for the surface intermediate (ΔG_r, kcal mol^{-1}) and the flux of the partial charge (q) at each step reaction in the constant potential method and the relevant energies in the neutral charge method corresponding to Fig. 5 (b) and Fig. 7. The CPCM model is applied in those computations and NO molecule is taken as reference, and q is defined according to eqn (SI-2) and (SI-4), respectively, for the adsorption and the reduction processes

	Constant potential method						Neutral charge method
	0 V		0.33 V		0.84 V		0 V
	ΔG_r	q	ΔG_r	q	ΔG_r	q	ΔG_r
*NO	-61.3786	-0.016	-59.7261	0.005	-57.8232	0.039	-61.1663
*NOH	-30.4745	0.169	-25.4957	0.176	-18.0211	0.187	-54.2950
*HNO	-24.4692	0.167	-18.8682	0.177	-25.5468	0.096	-53.6337
*N	-83.3762	0.056	-78.1771	-0.042	-67.1912	-0.194	-88.5050
*HNOH	-30.0924	0.155	-16.4979	0.163	-3.1214	0.143	-60.7714
*H_2NO	-12.7104	0.377	-6.0182	0.349	2.4514	0.308	-64.1571
*NH	-71.2848	0.221	-54.9128	0.195	-28.8467	0.156	-100.9995
*NH_2OH	-23.0023	0.386	-9.9075	0.349	11.4183	0.293	-73.6107
*NH_2	-78.5458	0.128	-50.4865	0.126	-7.0672	0.124	-110.5395
*NH_3	-58.2968	0.544	-30.6223	0.525	12.7052	0.496	-129.1182

Table S2 Activation energies (E_a, kcal mol^{-1}) for the N-H and the O-H bond formation via the LH and the ER mechanism, and the corresponding potentials for their initial and transition states in the constant charge method with the CPCM model on the Pt(111) surface of the Pt_{37} cluster

Mechanism	Charge	N-H (HNO)			O-H (NOH)		
		E_a	U_{int}	U_{ts}	E_a	U_{int}	U_{ts}
LH	0	15.21	0.680	0.696	31.19	0.701	0.718
	-1	15.44	0.514	0.513	30.60	0.531	0.540
	-2	16.90	0.341	0.343	30.88	0.367	0.366
ER	-1	22.19	0.507	0.531	18.82	0.552	0.529
	-2	19.55	0.350	0.361	18.52	0.400	0.366
	-3	19.77	0.198	0.186	20.19	0.220	0.180

Table S3 pK_a of the ground-state HNO and NOH in aqueous solution according to solvation energies calculated with the CPCM model in the different methods

Method	HNO	NOH
HF/6-31G*	13.20	-4.16
HF/6-31G**	13.23	-4.21
HF/def2-SVP	13.12	-4.34
HF/def2-TZVP	13.53	-3.83
HF/cc-pVDZ	13.52	-4.01
HF/cc-pVTZ	13.50	-4.01
B3LYP/6-31G*	14.39	-2.02
B3LYP/6-31**	14.38	-2.08
B3LYP/def2-SVP	14.03	-2.41
B3LYP/def2-TZVP	14.96	-1.55
B3LYP/cc-pVDZ	14.92	-1.67
B3LYP/cc-pVTZ	14.95	-1.73

Table S4 Bond length (d, Å), bond order (B) and bond angle (∠, º) of ground-state NOH and HNO in the gas phase and on the Pt_{37} cluster obtained at the B3LYP/def2-TZVP level of theory. Subscripts t and f stand for the top and the fcc sites of the Pt(111) surface, respectively

	d_{N-O}	B_{N-O}	d_{O-H}	B_{O-H}	d_{N-H}	B_{N-H}	$\angle_{NOH}$	$\angle_{HNO}$	d_{N-Pt}	B_{N-Pt}
NOH	1.321	1.207	0.975	0.854			109.28			
NOH_t	1.355	1.114	0.972	0.864			104.69		1.945	1.069
NOH_f	1.375	0.952	0.975	0.854			104.84		1.993 1.991 1.964	0.718 0.632 0.628
HNO	1.197	1.868			1.065	0.889		108.90		
HNO_t	1.201	1.595			1.039	0.827		115.98	1.952	1.054
NO^-	1.258	1.308								

Table S5 Standard potentials of O_2 reduction to H_2O in aqueous solution according to solvation energies calculated with the SMD model in the different methods

Method	H_2O	O_2^-
HF/6-31G*	1.34	-0.21
HF/def2-SVP	1.32	-0.21
HF/cc-pVDZ	1.31	-0.24
B3LYP/6-31G*	1.32	-0.34
B3LYP/def2-SVP	1.30	-0.32
B3LYP/cc-pVDZ	1.29	-0.39

Table S6 Potentials of NO reduction to the ground-state NO^-, NOH and HNO on the Pt(111) surface of the Pt_{37} cluster calculated in the indirect and the direct approaches

	Indirect			Direct	
Site	NO^-	NOH	HNO	NOH	HNO
top	-0.94	-1.14	-0.62	-1.39	-0.60
fcc	-4.35	--	--	-4.40	--

Reference

1. U. Benedikt, W. B. Schneider and A. A. Auer, *Physical Chemistry Chemical Physics*, 2013, **15**, 2712-2724.
2. J. Rossmeisl, J. K. Nørskov, C. D. Taylor, M. J. Janik and M. Neurock, *The Journal of Physical Chemistry B*, 2006, **110**, 21833-21839.